

Atomistic Simulations of CO₂ and N₂ Adsorption in Silica Zeolites: The Impact of Pore Size and Shape[†]

Anne Goj,[‡] David S. Sholl,^{§,⊥} E. Demet Akten,[§] and Daniela Kohen^{*,||}

Chemistry Department, Smith College, Northampton, Massachusetts 01063, Department of Chemical Engineering, Carnegie Mellon University, Pittsburgh, Pennsylvania 15213, Chemistry Department, Carleton College, Northfield, Minnesota 55057, and National Energy Technology Laboratory, Pittsburgh, Pennsylvania 15236

Received: April 4, 2002; In Final Form: June 10, 2002

Adsorption of CO₂ and N₂, both as single components and as binary mixtures, in three zeolites with identical chemical composition but differing pore structures (silicalite, ITQ-3, and ITQ-7) was studied using atomistic simulations. These three zeolites preferentially adsorb CO₂ over N₂ during both single-component and mixture adsorption. The CO₂/N₂ selectivities observed in the three siliceous zeolites vary strongly as the adsorbent's crystal structure changes, with the selectivity in ITQ-3 being the largest. Our studies indicate that the different electric fields present inside zeolites with different crystal structures but identical chemical composition play an important role in the observed adsorption capacities and selectivities. The accuracy of the ideal adsorbed solution theory in predicting the behavior of CO₂/N₂ mixtures in silica zeolites based on single component adsorption data was also tested; this theory performs quite accurately for these adsorbed mixtures.

1. Introduction

The adsorption of gases inside crystalline microporous materials is the basis of many industrial processes for gas purification and separation.¹ As part of efforts to reduce emission of greenhouse gases, it has recently been suggested to use microporous adsorbents to selectively remove CO₂ from gas streams.² To explore the feasibility of this process, Siriwardane et al. have measured the adsorption of CO₂, N₂, H₂ and their mixtures on two zeolites, 13X and 4A.² These experiments showed that CO₂ is selectively adsorbed in these zeolites relative to N₂ and H₂ over a broad range of pressures at room temperature. In pursuing practical applications and given the huge variety of known zeolite structures it is naturally desirable to select materials that have the most favorable adsorption characteristics. To guide this process, it would be useful if insight were available into what features of zeolite structure control the adsorption properties of quadrupolar species such as CO₂ and N₂.

In this paper, we use atomistic modeling to study the adsorption of CO₂ and N₂, both as single components and as binary mixtures, in three zeolites with identical chemical composition but differing pore structures, silicalite, ITQ-3, and ITQ-7. Although there is a considerable body of work on simulating adsorption in zeolites with atomistic methods, as reviewed recently by Fuchs and Cheetham,³ there have only been a small number of studies investigating quadrupolar species. There have been no previous studies of CO₂/N₂ mixture adsorption or studies that systematically examine the properties of these adsorbates in a series of zeolite structures.

Almost all practical applications of zeolites as adsorbents involve their behavior when contacted with gas mixtures. Unfortunately, determining equilibrium adsorption data for multicomponent mixtures is much more challenging than measuring the equivalent single-component data.⁴ In the work of Siriwardane et al., for example, single-component adsorption isotherms are directly measured but the properties of gas mixtures are only examined indirectly through dynamic studies with a microreactor.² In practical applications, binary adsorption data is typically predicted from single-component adsorption measurements using approximate methods such as the ideal adsorbed solution theory (IAST).¹ Evaluation of the accuracy of IAST using experimental data has been performed for a number of systems. In some cases IAST is quantitatively accurate, but in other cases there are significant discrepancies between IAST and the true multicomponent isotherms.¹ It is important to have an accurate description of multicomponent adsorption data because these data are critical input for the design of large-scale adsorption processes.⁵ Even though the majority of atomistic simulations of adsorption in zeolites have focused on single-component adsorption³, an important role for atomistic simulations is to examine multicomponent adsorption. Several studies have used atomistic simulations to directly generate equilibrium binary adsorption data and use these data to test the accuracy of IAST.^{6–8} Below we use our simulation data for CO₂ and N₂ adsorption in silica zeolites to examine the accuracy of IAST for these systems.

The paper is organized as follows. In section 2 we describe the structure of the three silica zeolites we have studied, as well as the interatomic potentials we used to model CO₂ and N₂ adsorption in these zeolites. We also summarize our simulation methods, paying particular attention to the techniques we have used to efficiently deal with electrostatic interactions. In section 3 we describe the single-component adsorption of CO₂ and N₂ in silicalite, ITQ-3, and ITQ-7 at room temperature and elevated temperatures. These data are extended to binary mixtures of

[†] Part of the special issue "John C. Tully Festschrift".

^{*} Corresponding author. Fax: (507) 646 4400. E-mail: dkohen@carleton.edu.

[‡] Smith College.

[§] Carnegie Mellon University.

^{||} Carleton College.

[⊥] National Energy Technology Laboratory.

TABLE 1: Potential Parameters Used to Represent the Zeolite Frameworks and Guest Molecules

		LJ parameters			partial charges (e)
		ϵ/k_b (K)	σ (Å)	$r_{\text{cut-off}}$	
zeolites	Si	0.0			+2
	O	89.6	2.806	9.0	−1
CO ₂ (C–O distance: 1.16 Å)	C	27.0	2.80	9.0	+0.7
	O	79.0	3.05	9.0	−0.35
N ₂ (N–CofM distance: 0.55 Å)	N	36.0	3.31	10.0	−0.482
	CofM	0.0			+0.964

CO₂ and N₂, and the results of our direct atomistic simulations are compared with the predictions of IAST. We conclude in section 4 by discussing how the differing adsorption characteristics of the three zeolites we have examined are influenced by their pore geometry.

2. Methods and Models

2.1. Atomistic Models for CO₂ and N₂ in Silica Zeolites.

To facilitate comparison between several zeolites with differing pore geometries, we have chosen to study three siliceous zeolites: silicalite, ITQ-3, and ITQ-7. The simple chemical composition of these zeolites (SiO₂) is convenient for atomistic modeling because it requires fewer interatomic potential parameters than cationic aluminosilicate zeolites. As in most previous atomistic studies of adsorption in zeolites, we assume the adsorbent can be treated as a rigid framework with atomic positions fixed by the observed crystallographic data.³ This approximation is known to be problematic for some guest molecules that are extremely tightly confined in zeolite pores,⁹ but this is not the case for the guest/host systems studied here.

Silicalite (structure type MFI), the all-silica isomorph of ZSM-5, has been extensively studied both experimentally^{10–13} and theoretically.^{3,7,14–18} We examined silicalite in its orthorhombic form as described previously.¹⁸ The structure of silicalite's pores is well known; it has two sets of interconnected 10-ring pores about 5.5 Å in diameter. The straight and sinusoidal channels intersect at right angles, with the channel intersections being slightly larger than the channels themselves.¹⁹ The density of silicalite is 1.79 g/cm³.¹⁹ ITQ-3²⁰ and ITQ-7²¹ are two newer siliceous materials. ITQ-7 (structure type ISV) has a three-dimensional system of large pores defined by windows containing 12-member rings of about 6 Å in diameter, and therefore it has a lower framework density than silicalite (1.54 g/cm³) and a high void space. ITQ-3 (structure type ITE), on the other hand, has a one-dimensional pore system with small windows of about 4 Å in diameter made up of 8-member rings that open to larger cavities. A second straight channel runs through the material but is too narrow to accommodate guest molecules. The density of ITQ-3, 1.63 g/cm³, is intermediate between the densities of silicalite and ITQ-7. We used the atomic coordinates reported for calcined ITQ-7 by Villaescusa et al.²¹ and for calcined ITQ-3 by Camblor et al.²⁰

We modeled interactions between adsorbed molecules and the zeolite framework atoms following the method of Makrodimitris et al.¹⁷ That is, each O atom in the zeolite is assumed to interact with each site on adsorbed molecules through both a Lennard-Jones potential and electrostatic interactions, while only electrostatic interactions are considered between adsorbates and Si atoms in the zeolite. We have used the parameters reported by Makrodimitris et al.¹⁷ as model LJCB.JBTLC^{22,23,16} (see Table 1 for all parameters) because this model was successful in reproducing experimental isotherms for N₂ and

CO₂ on silicalite at room temperature (see below). An important assumption in our work is that potential parameters can be transferred directly to model the same molecules adsorbed in ITQ-3 and ITQ-7. This approach seems plausible because each material has precisely the same composition, but given the absence of experimental adsorption data in these two materials, we are unable to directly assess the validity of this assumption.

Carbon dioxide was modeled as a linear triatomic and nitrogen as a diatomic molecule with fixed bond lengths and bond angles. Both species were modeled by charged Lennard-Jones (LJ) centers using the TraPPE force field developed by Potoff and Siepmann.²⁴ These potentials quantitatively reproduce the vapor–liquid equilibria of the neat systems and their mixture. In this model, partial point charges are centered on each LJ site (and additionally at the molecule's center of mass in the case of N₂) to approximate the first order electrostatic and second order induction interactions, and only nonbonded atoms interact with each other. This model is very similar to other models that have been used in the past to describe these species.²⁵ LJ parameters for the unlike-pair interactions are calculated with the widely used Lorentz–Berthelot combining rules.²⁶ Special efforts were taken in the construction of the TraPPE potential to incorporate this last feature as it increases the transferability of the force fields. This makes the TraPPE model especially attractive when using it to describe the interaction of the sorbate molecules with other species. These same combining rules were used to calculate the LJ parameters describing the interaction of the guest molecules with the zeolite frameworks. Long-range corrections to the LJ potentials were included, these corrections were calculated assuming a uniform distribution of particles beyond the cutoff distances of each atom in the simulation cell.

2.2. Simulation Methods. Single component and mixture adsorption simulations were carried out using the grand canonical Monte Carlo (GCMC) method.^{3,27} In our GCMC simulations three types of trial moves were used: attempts to insert a new molecule in the zeolite, attempts to delete an existing molecule from the zeolite, and attempts to move an adsorbed molecule. For the creation attempt, the algorithm due to Marsaglia²⁸ was used to ensure a random position and orientation of the trial molecule. Attempts to move molecules within the zeolite consisted of either a rigid body translation or a rotation of the molecule about its center of mass and one of the three space-fixed axes.²⁶ Typically single-component simulations were run for about 5×10^6 Monte Carlo moves, while simulations of mixtures were run for 6×10^6 Monte Carlo moves. In both cases the first half of these moves were used for equilibration and were not included in the averaging. The chemical potential of the bulk gas phase in our single-component calculations was related to the gas pressure using the BWR equation of state.²⁹ In our binary mixture calculations, the mixtures were treated as ideal but the partial pressure of each gas was calculated using the BWR equation of state.

Two different methods were used to assess the statistical uncertainties in our GCMC calculations. First, results were computed sequentially for both adsorption, that is, increasing pressure after the completion of each simulation, and desorption. In the next section both adsorption and desorption isotherms are shown. The degree of overlap of these two independent calculations gives an indication of the consistency of our results and the adequacy of our equilibration methods. Second, at each pressure considered, each simulation was divided into 10 blocks, and the standard deviation of these block averages was

calculated.²⁷ These standard deviations were used while propagating errors when estimating the uncertainty in adsorption selectivities.

In addition to calculating the equilibrium pore loading at each set of bulk phase conditions we considered, we also computed isosteric heats of adsorption, Q_{st} . To calculate Q_{st} for the interaction of the zeolites with pure gases, the method of Karavias and Myers³⁰ was followed. Q_{st} can be calculated as the difference of the partial molar enthalpy of the sorbate in the bulk phase and partial molar internal energy in the adsorbed phase.³¹ Assuming ideal behavior in the bulk phase, the isosteric heat for component i of a mixture can thus be calculated as³⁰

$$Q_{st}^i = RT - \left(\frac{\partial U}{\partial n_i} \right)_{T,V,n_j \neq n_i}$$

where U is the internal energy of the sorbate in the adsorbed phase. U is the sum of the interactions of all adsorbed species among themselves and with the zeolite. The partial derivative can be determined in GCMC simulations in terms of fluctuations in the internal energy and number of adsorbed molecules.^{30–32} Note that in these calculations the assumption is that the bulk gas behaves ideally, while elsewhere in this work the BWR equation of state has been used to describe the behavior of the pure gases. At the pressures studied here, assuming that the gases are ideal should result in a slight underestimation of the calculated isosteric heats.

As it is mentioned above, both host/guest and guest/guest interactions were modeled by the sum of short-range interaction terms using Lennard-Jones potentials and Coulombic terms accounting for the long-range interaction between the quadrupole moment of the guests and the zeolite's electrostatic field. In all simulations the simulation box was chosen as containing the smallest number of zeolite unit cells such that its shorter side was longer than twice the largest Lennard-Jones cutoff. Periodic boundaries and the minimum image convention were used to properly deal with the short-range interactions. To properly treat the long-range interactions among guest molecules, the Ewald summation method was used.^{28,33} The width of the Gaussian distributions that constitute the screening charges in this method, κ , as well as the number of wave vectors necessary to represent the interaction in reciprocal space were optimized to correctly reproduce values obtained using an "infinitely" large cell (see below). In most simulations, 276 wave vectors were used, and κ was equal to $6/\bar{L}$, where \bar{L} is the average length of the simulation box. A useful property of an arbitrary collection of quadrupolar molecules is that their total dipole moment is exactly zero. As a result, there is no need to specify the nature of the medium surrounding the system as there is in periodic systems with nonzero dipole moments.³³

In principle, the Ewald summation could also be used to determine the total electrostatic interactions between quadrupolar guests and the zeolite framework. A much more numerically efficient scheme can be developed by noting that the electrostatic field due to the zeolite is independent of the adsorbate configuration since we have assumed the zeolite framework to be rigid. We therefore precalculate the electrostatic potential felt by a test charge located on a fine grid of points throughout the zeolite unit cell as a result of its interaction with an "infinite" zeolite.¹⁷ In the calculations below, we used a cubic grid with spacing 0.2 Å. To simulate an "infinite" cell, concentric consecutive layers of unit cells surrounded the central unit cell containing the test charge until convergence is attained. We found that excellent convergence could be achieved provided

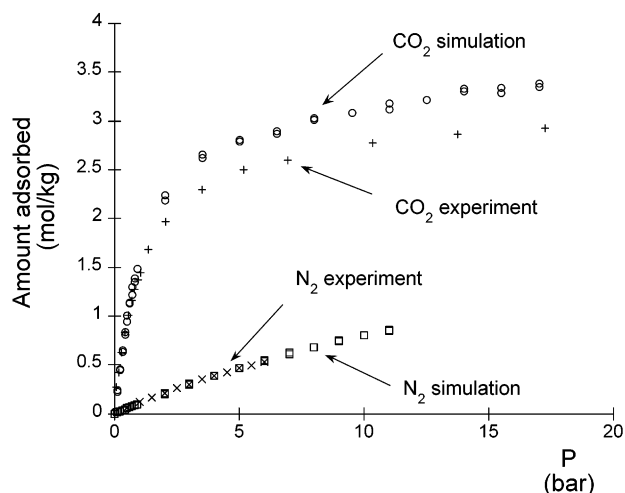


Figure 1. Single-component adsorption isotherms for CO₂ on silicalite at 308 K and N₂ on silicalite at 298 K as computed from GCMC and observed experimentally.

that two conditions were met. First, the net dipole moment of the zeolite framework in the central unit cell had to vanish. This condition can be met for each of the three zeolites we examined, provided care is taken in choosing the boundaries of the unit cell. Second, the electrostatic potential due to Si and O atoms must be considered simultaneously, not separately. If this approach is taken, convergence is greatly aided by the screening of charges that occurs at long distances in a charge neutral system. Once these conditions were satisfied, only 10 layers were necessary to achieve good convergence. The storage requirements for tabulating these electrostatic potentials were reduced by exploiting the symmetry of the unit cells in each material. Once this pretabulation was complete, a cubic interpolation scheme was used to evaluate the Coulombic potential felt by a given partial charge of a guest molecule. This interpolation scheme was reliable except in the strongly repulsive regions where the strength of the interaction tends to be overestimated. Since these regions make only negligible contributions to the thermodynamic properties of adsorption, this overestimation is of no consequence for our results.

2.3. Validation of the Models and Simulation Methods.

Adsorption of pure N₂ and pure CO₂ in silicalite has been previously studied, both experimentally^{10,11,34} and with numerical simulations.^{14,17,34} We have used this information to validate our choices of models and simulation methods. Figure 1 shows our GCMC results at 308 K for single-component adsorption on silicalite as well as results for N₂³⁴ and Sun's results for CO₂.¹¹ Reasonably good agreement is obtained for both adsorbates. The agreement is quantitative for N₂, and although the agreement is less remarkable for CO₂ it is good enough to warrant the use of the potentials and methods described earlier. Above it was mentioned that Makrodimitris et al.¹⁷ found good agreement between experimental and numerical simulations of CO₂ and N₂ isotherms. Under the wider range of pressures studied here, however, using their potential does not result in a significant improvement compared to using the one chosen for this work. Recall that the adsorbate–adsorbate parameters used here are not the same as the ones used by Makrodimitris et al., only the zeolite parameters are the same. With the goal of improving the agreement in the CO₂ isotherms we explored a number of alternative values for the framework oxygen Lennard-Jones parameters while holding fixed the partial charges of the zeolite. Although it was possible to improve the agreement with the experimental data at high pressures, this came at the cost of

significantly worsening the agreement in the Henry's law region of low pressures. The parameters summarized in Table 1 therefore appear to provide a reasonable means of describing CO₂ adsorption in silicalite over a broad range of pressures.

In Figure 1 we have followed the common practice of comparing absolute adsorbed amounts determined from simulations with excess adsorbed amounts determined from experiments.^{12,17} Talu and Myers have recently pointed out that it is more precise to correct the simulated result to mimic experimental measurements before making this type of comparison.³⁵ They determined that an appropriate correction for silicalite is to relate the excess adsorbed amount, N^{excess} , to the absolute adsorbed amount, N^{absolute} , by

$$N^{\text{excess}} = N^{\text{absolute}} - 175\rho_{\text{gas}}$$

where the adsorbed amounts are measured in mol adsorbed/kg adsorbent, and ρ_{gas} is the density of the gas phase in mol/cm³. At gas pressures of 10 bar, this correction is 0.068 mol/kg for the temperature used in Figure 1 if the gas phase is assumed to be ideal. Thus, this correction is negligible for the CO₂ data shown in Figure 1. Throughout the remainder of this paper, all adsorption data are reported in terms of absolute adsorption.

It is worth mentioning that Miyamoto et al.¹⁴ have reported a better agreement between their simulation results and experimental data for CO₂ than the agreement we report here. In Miyamoto's work, the charges on the zeolite atoms were optimized (resulting in values of 0.8e for Si and -0.40e for O) to fit the experimentally observed heat of adsorption for CO₂. In contrast, the partial charge values (-1.0e for O and +2.0e for Si) chosen by Makrodimitris et al.¹⁷ were based on semiempirical and local density functional theory electronic embedded-cluster calculations.^{22,23} This more rigorous approach strongly suggests that partial charges of this or similar size are reasonable for silica zeolite frameworks and should therefore not be treated as free parameters in determining interatomic potentials in these systems. Also, our choice of partial charges is supported by recent work on zeolites NaX,³⁶ mordenite,³⁷ and faujasite-type³⁸ since in all these different materials partial charges with values very similar to 2.0e for Si and -1e for O have been successfully used. This leads us to prefer the potentials of Makrodimitris et al. for adsorbate-zeolite interactions to those of Miyamoto et al., despite the slightly better agreement with measured isotherm data seen by the latter.

Isosteric heats of adsorption of CO₂ and N₂ on silicalite calculated using experimental isotherms have been reported as well; this allowed an additional check of our methods and models. Golden et al.¹⁰ report a value of 24.07 kJ/mol for CO₂ and 15.07 kJ/mol for N₂ in the limit of zero loading. The same authors report that between 0 and 7 atm these values increase slightly, by no more than 5%. Sun et al.¹¹ report values of about 28.5 kJ/mol for CO₂ loadings up to 2.5 mol/kg. Note that the method these authors used to calculate Q_{st} gives temperature-independent values. Using our numerical simulations at room temperature (see below) we obtain, for the pressures studied, Q_{st} for CO₂ on silicalite of 25–30 kJ/mol and 13.5–15 kJ/mol for N₂ on silicalite. Numerical simulations at 498 K (see below) show that these results do not change much with temperature. We conclude from these data that our atomistic model is in good agreement with the available experimental data for single component adsorption of CO₂ and N₂ on silicalite.

2.4. Ideal Adsorbed Solution Theory. Ideal adsorbed solution theory (IAST) is a simple technique for predicting the adsorption equilibria for components in a multicomponent mixture using only data from the pure-component adsorption

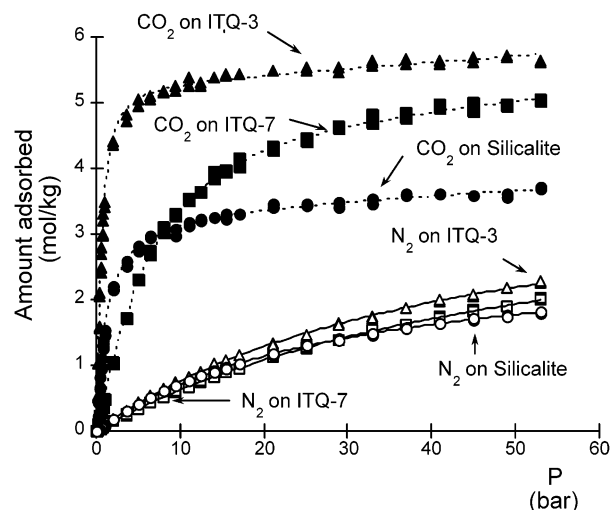


Figure 2. Single-component adsorption isotherms for CO₂ (filled symbols) and N₂ (unfilled symbols) on silicalite (circles), ITQ-3 (triangles), and ITQ-7 (squares) at 308 K as computed from GCMC. Adsorption and desorption isotherms are shown for both N₂ and CO₂.

equilibria at the same temperature on the same adsorbent.^{1,39} The implicit assumption of IAST is that the adsorbate mixture behaves as an ideal solution.³⁹ IAST is an analogue of Raoult's law for vapor/liquid equilibria, but instead of relating the molar fraction of the solute i in solution (x_i) to its partial pressure in the gas phase (P_i), IAST relates the molar fraction of i in the adsorbed phase (also x_i) to its partial pressure in the gas phase. Below, we apply IAST to predict the binary equilibrium isotherms of CO₂/N₂ mixtures in silicalite, ITQ-3, and ITQ-7 based on the single-component isotherms determined in our GCMC calculations and examine the accuracy of these predictions by directly comparing them to multicomponent GCMC simulations. To do this, our single-component isotherms must be fitted to a continuous function to allow the numerical solution of the equations arising in IAST. In the work presented in this paper, the single-component adsorption isotherms were fitted either to a Langmuir form

$$n(P) = \frac{K_H P}{1 + BP}$$

or, when a Langmuir fit was not adequate, to an isotherm described by Jensen and Seaton,⁴⁰

$$n(P) = K_H P \left\{ 1 + \left(\frac{K_H P}{\alpha(1 + \kappa P)} \right)^C \right\}^{-1/C}$$

3. Results and Discussion

3.1. Single Component Adsorption. The isotherms computed from our single-component GCMC calculations for CO₂ and N₂ in silicalite, ITQ-3, and ITQ-7 at 308 K are shown in Figure 2. No hysteresis is seen in any of these examples. As was already seen in the experimental data for silicalite in Figure 1, these materials strongly adsorb CO₂ relative to N₂. Siriwardane et al. have also observed this qualitative result in their experiments with the cationic zeolites 13X and 4A².

The stronger adsorption of CO₂ in these materials can also be inferred from the potential parameters summarized in Table 1. The dispersion interactions for the CO₂ and N₂ interacting with the silica zeolites are quite similar. Since the quadrupole moment of CO₂ is about three times larger than that of N₂, the former species interacts more strongly with the electrostatic field defined by the zeolites. While the amount of N₂ adsorbed in

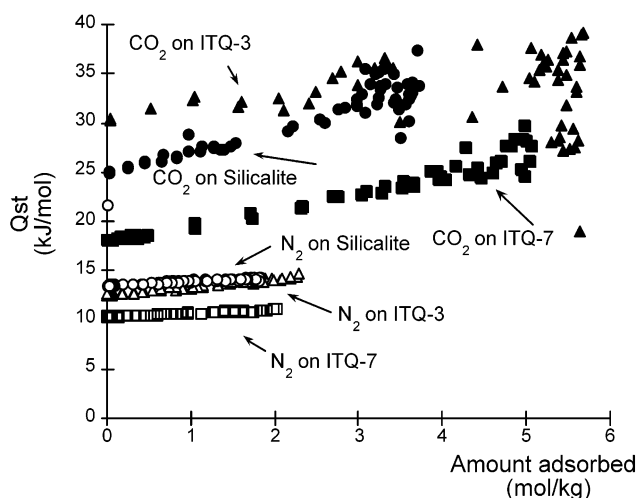
TABLE 2: Fit Parameters for Single-Component Simulations

Langmuir Fits: $K_H P / (1 + BP)$						
temperature (K)	sorbate	sorbent	K_H (mol/kg bar)	B (1/bar)		
308	N ₂	ITQ-3	0.0935	0.0227		
		ITQ-7	0.0739	0.0182		
		silicalite	0.0962	0.0343		
498	N ₂	ITQ-3	0.0145	0.0046		
		ITQ-7	0.0150	0.0040		
		silicalite	0.0123	0.0046		
	CO ₂	ITQ-3	0.0731	0.0156		
		ITQ-7	0.0392	0.0091		
		silicalite	0.0575	0.0206		
Jensen and Seaton Fits: $K_H P \{1 + (K_H P / \alpha (1 + \kappa P))^C\}^{-1/C}$						
temperature (K)	sorbate	sorbent	K_H (mol/kg bar)	α (mol/kg)	κ (1/bar)	c
308	CO ₂	ITQ-3	6.1	5.26	0.0017	1.5
		ITQ-7	0.56	4.7	0.0021	1.6
		silicalite	2.59	3.40	0.0020	1.07

each of the three materials we examined is quite similar over the range of pressures shown in Figure 2, there are substantial differences between the CO₂ isotherms in the three zeolites. ITQ-3 adsorbs CO₂ strongly, even at low pressures. Silicalite adsorbs CO₂ almost as strongly at low pressures but can accommodate fewer guest molecules at high pressures. ITQ-7 adsorbs the least CO₂ of these three zeolites at low pressures, but shows a higher saturation loading than silicalite.

Figure 2 shows not only the results of our GCMC simulations (symbols) but also our best fits to these adsorption isotherms. Fits to the single-component isotherms are necessary to predict the behavior of the gas mixtures using IAST. Langmuir isotherms adequately fit the nitrogen isotherm (full lines) but did not give satisfactory fits for any of these CO₂ results. Fitting the CO₂ isotherms with a Langmuir–Freundlich equation for nonuniform surfaces¹ or with the Toth equation^{40,12} did not result in substantially better fits, but using the isotherm proposed by Jensen and Seaton (see above) was satisfactory. The fits obtained using the Jensen and Seaton form are shown in Figure 2 as dashed lines. The fitting parameters for each N₂ and CO₂ isotherm are summarized in Table 2.

It is interesting to study the correlation of CO₂ loading in the saturation limit in the different materials with their density or pore size, as a very simple explanation of the trend could lie in the materials void space. Our simulations show that ITQ-3 is the material with the largest capacity of CO₂ with a saturation limit of approximately 5.7 mol/kg, ITQ-7 is next with 5 mol/kg and ITQ-3 with 3.7 mol/kg is last. In contrast, ITQ-3 pores are 4 Å, ITQ-7 pores are 6 Å, and silicalite pores are 5.5 Å. Clearly the pore size is not a predictor of the material's adsorption capacity. This lack of correlation can be understood by noting that the size of a pore is not correlated in a simple way to the size of the cavities it is connecting. To investigate the correlation between saturation loading and void space (on a mass basis), we estimated this second quantity in the different zeolites. To do so we first calculated the percent of the unit cell volume that was available to CO₂ molecules by selecting 10⁶ points at random within each unit cell, locating the C atom of a CO₂ molecule on each of these sites, and then calculating the total energy of the site for 20 different random orientations of the guest molecule. If any of these configurations was stable (a negative total energy) then the site was considered an attractive site. To estimate the percentage of the unit cell volume that was available to CO₂ molecules, we simply divide the number

**Figure 3.** Isosteric heats of adsorption for single component adsorption of CO₂ and N₂ on silicalite, ITQ-3, and ITQ-7 at 308 K as computed from GCMC. The same symbols are used as in Figure 2.

of attractive sites by the total number of sites considered. To calculate the void space per kilogram, we divided this last quantity by the density of the materials. ITQ-3, the material with the largest saturation loading and the one that reaches this limit at lowest bulk pressures, has an available space of 0.11 cm³/g; ITQ-7, the material with a saturation loading almost as large as that of ITQ-3, has an available space of 0.15 cm³/g; and silicalite has an available space of 0.08 cm³/g. The material with the lowest void space (silicalite) is the one with the minimum capacity, as expected. On the other hand, the ITQ-3 and ITQ-7 order is reversed. This reversal may be only apparent since the conclusion reached above that ITQ-3 has a marginally larger saturation loading than ITQ-7 relies on the range of pressures studied; it is possible that at higher pressures this might change. Another possibility is that for these materials the nature of the packing of guest molecules is such that site availability changes dramatically when other guest molecules are occupying neighboring sites, in which case we cannot expect a good correlation between the loading at the saturation limit and the available void space.

The isosteric heat of adsorption for single-component CO₂ and N₂ at 308 K in the three silica materials we have studied is shown in Figure 3. Consistent with the isotherms shown in Figure 2, CO₂ exhibits the highest isosteric heat of adsorption in ITQ-3 and the lowest in ITQ-7. The latter observation reinforces the comment above that the saturation loading of CO₂ in ITQ-7 is higher than silicalite simply because of ITQ-7's larger available pore volume rather than the presence of stronger CO₂–zeolite interactions at high pore loadings. In all three materials, the isosteric heat of adsorption increases weakly with pore loading, indicating that the adsorption sites in each material are reasonably homogeneous. The increase in Q_{st} with loading can be attributed to an increase in the guest/guest interactions. The isosteric heats of adsorption for N₂ in silicalite, ITQ-3, and ITQ-7 are quite similar and, consistent with the adsorption isotherms shown in Figure 2, significantly smaller than those of CO₂. The fluctuation-based methods we used to compute Q_{st} led to considerable scatter in the data at loadings approaching the saturation loading of the species being considered, as can be seen in Figure 3.

In a number of practical applications where CO₂-selective adsorption could be used as part of a CO₂-sequestration strategy, such as coal gasification or natural gas reforming, mixed gas streams exist at elevated temperatures. It is therefore interesting

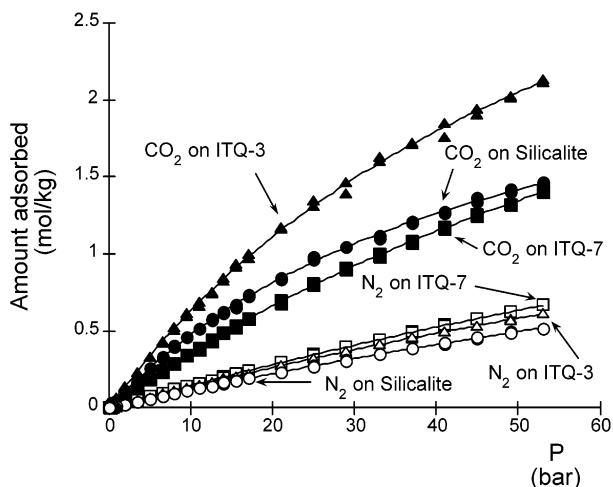


Figure 4. The same as Figure 2 but for single component adsorption at 498 K.

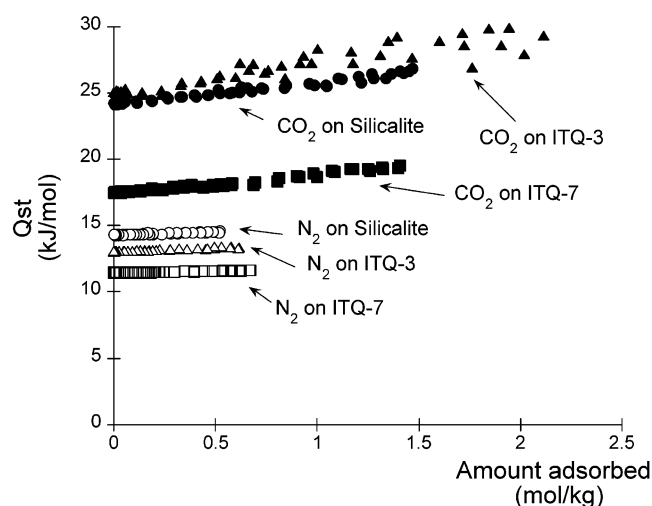


Figure 5. The same as Figure 3 but for adsorption at 498 K.

to investigate how microporous adsorbents would adsorb CO_2 not only around room temperature but also at higher temperatures. Figures 4 and 5 are equivalent to Figures 2 and 3 but show results obtained at 498 K. All the isotherms were adequately fitted by Langmuir isotherms (solid lines). These plots show the same qualitative behaviors as at room temperature, but in all cases adsorption is weaker and the quantitative differences between the three materials are less distinct.

We conclude our discussion of single-component adsorption by returning to the relative importance of dispersive versus electrostatic forces in controlling adsorption in these materials. To probe this issue, we computed single-component isotherms at 308 K as above but with the partial charges on each adsorbing molecule set artificially to zero. That is, we performed GCMC simulations using the same potential parameters as in the calculations shown in Figures 2 and 3, but included only dispersion interactions. The results of simulations at room temperature are displayed in Figure 6a, b. The scale in these plots is the same as in Figures 2 and 3. The differences in the behavior of nitrogen in all three materials are minimal, consistent with the small quadrupole moment of this molecule. On the other hand, the differences in the adsorption behavior of carbon dioxide are substantial. When comparing the CO_2 isotherms (Figures 2 and 6a) and isosteric heats of adsorption (Figures 3 and 6b), two features are immediately apparent: (1) in all cases the carbon dioxide adsorption is significantly weaker in the

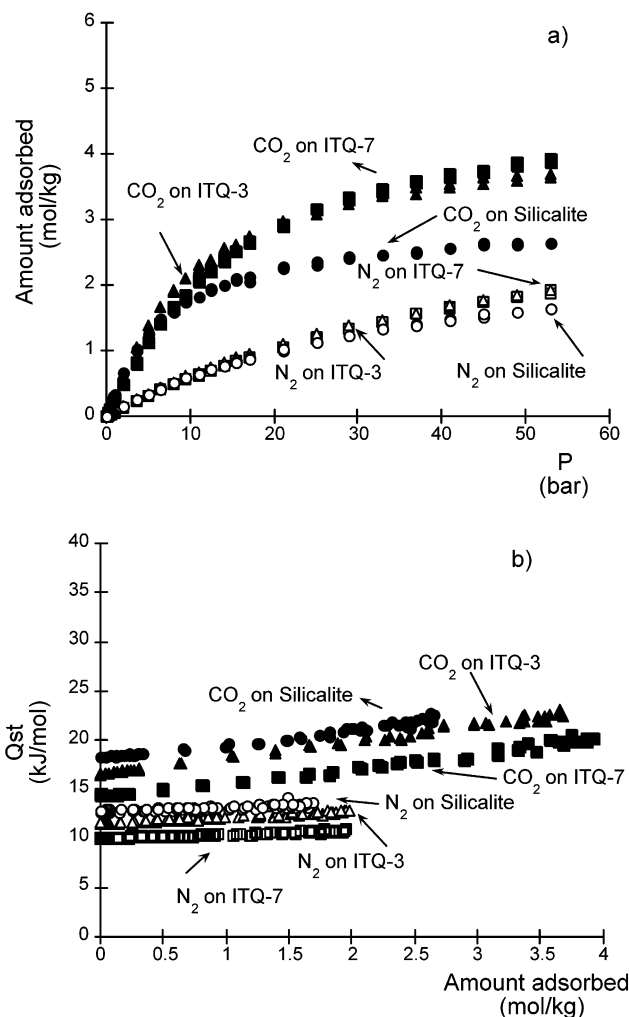


Figure 6. GCMC results for single-component adsorption of CO_2 and N_2 on silicalite, ITQ-3, and ITQ-7 when only dispersive interactions are considered. Results are shown for (a) adsorption isotherms and (b) Q_{st} using the same symbols as in Figure 2.

absence of Coulombic interactions and (2) the behavior of CO_2 in ITQ-3 and ITQ-7 becomes quite similar when Coulombic interactions are not taken into account. The first feature was completely expected given the relatively large quadrupole moment of carbon dioxide. The second one was more surprising, but can be rationalized by considering the relative range of the dispersive and electrostatic potentials created by the zeolite frameworks. The strength of the dispersive potential is mainly determined by the spacing and density of O atoms in the zeolite framework near an adsorbed molecule, so this potential is not strongly affected by the large-scale structure of the crystalline material in a series of materials with the same chemical composition and similar densities. The electrostatic potential, in contrast, is a long-range potential and is therefore more sensitive to the large-scale structure of the crystalline adsorbent. Unfortunately, this argument seems to be useful only in a qualitative sense; there does not seem to be any straightforward way to apply it to the question of which material would show stronger interactions with quadrupolar adsorbates without performing the detailed calculations of the total electrostatic potential that are necessary for our GCMC calculations.

3.2. Mixture Adsorption. All three materials studied selectively absorb CO_2 relative to N_2 . Figure 7 shows the behavior of an equimolar CO_2/N_2 bulk mixture in the materials studied at 308 K. The symbols represent the mole fraction of CO_2 (filled

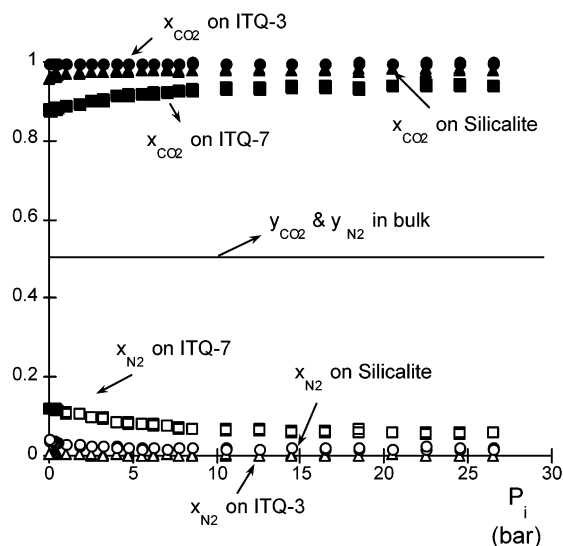


Figure 7. Mole fractions of adsorbed CO₂ and N₂ on silicalite, ITQ-3, and ITQ-7 at 308 K in equilibrium with an equimolar bulk mixture as computed using GCMC. The same symbols are used as in Figure 2.

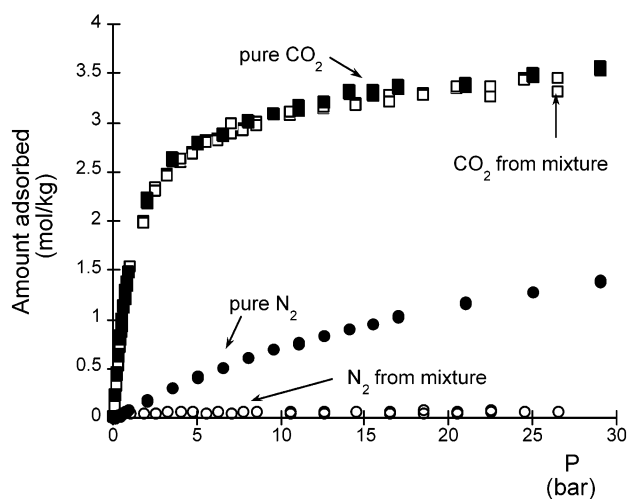


Figure 8. Comparison of single-component (filled symbols) and binary mixture (unfilled symbols) adsorption isotherms for silicalite at 308 K as computed from GCMC. The mixture isotherm is for an equimolar bulk gas mixture.

symbols) and N₂ (unfilled symbols) in the zeolite while the solid line represents the mole fraction of CO₂ and N₂ in the bulk. The horizontal axis corresponds to partial pressure of each bulk species. In each material and at all pressures a large majority of the adsorbed molecules are carbon dioxide, an expected result given the behavior of the pure gases in these zeolites. Also, in all cases as the pressure increases the adsorbed molar fraction of CO₂ increases, indicating that carbon dioxide molecules are displacing the less strongly adsorbed nitrogen molecules. Comparing the single-component isotherms to their counterparts in the mixture is interesting. Figure 8 shows this comparison when the zeolite is silicalite. Very similar results are observed for ITQ-3 and ITQ-7 (data not shown). Note how even though the behavior of carbon dioxide seems almost unaffected by the presence of nitrogen, the difference in the behavior of nitrogen is quite remarkable as the capacity of the zeolite to adsorb it is extremely diminished by the presence of adsorbed CO₂.

Plots of the adsorption selectivity of the three materials have been considered best display their ability to selectively adsorb CO₂ in the presence of N₂ (Figures 9–11). Selectivity is defined as the ratio of adsorbed molar fraction (x) over bulk molar

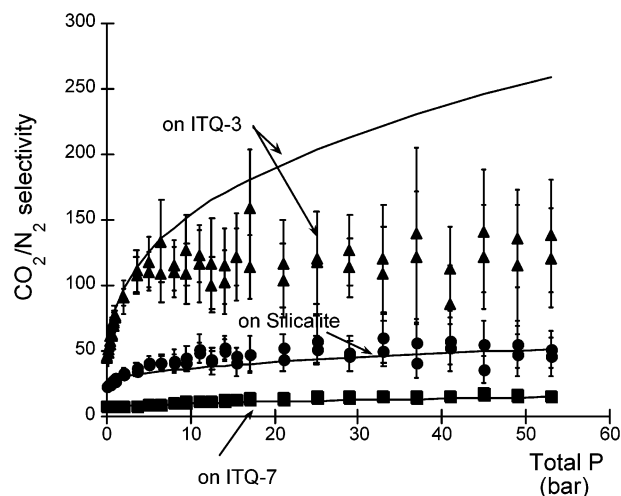


Figure 9. CO₂/N₂ selectivity from an equimolar bulk mixture on silicalite (circles), ITQ-3 (triangles), and ITQ-7 (squares) at 308 K. The data points are from GCMC and the solid curves are the predictions of IAST.

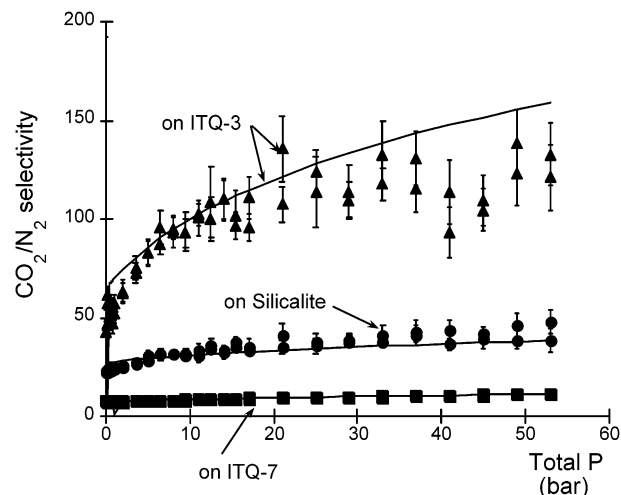


Figure 10. The same as Figure 9 but for a 90:10 N₂/CO₂ bulk mixture.

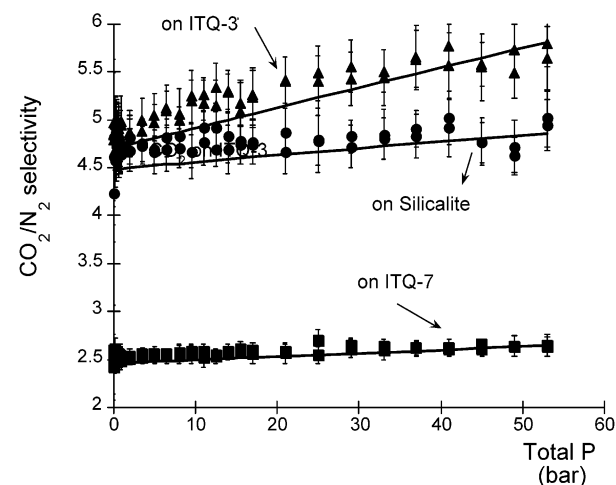


Figure 11. The same as Figure 9 but at 498 K.

fraction (y) of one material over the other, $S_{\alpha/\beta} = (x_{\alpha}/x_{\beta})(y_{\beta}/y_{\alpha})$. This quantity can easily be calculated using results from mixture GCMC simulations as well as using IAST. The latter method is based on results from our single-component GCMC simulations. Figure 9 shows both mixture GCMC results (symbols) and IAST results (lines) for an equimolar bulk mixture

at 308 K. Figure 10 shows equivalent results regarding a 0.9 N₂/0.1 CO₂ bulk mixture at 308 K, and Figure 11 an equimolar bulk mixture at 498 K.

In general, the agreement between IAST and our binary GCMC simulations is very good. In the limit of low pressures, the assumptions of IAST become exact, so precise agreement between IAST and mixture GCMC is to be expected. Indeed, the selectivity in this limit is simply the ratio of the Henry's law constants for the two adsorbed species, a result that is independent of the bulk phase composition.⁸ Inspection of Figures 9–11 shows some differences between IAST and the mixture GCMC data in the limit of low pressure. These deviations are due to the inability of our fitted single component isotherms to exactly capture the Henry's law constants, a difficulty that also exists when applying IAST to experimental data. Comparison of Figures 9 and 10 indicates that in each microporous material we have examined, the CO₂/N₂ selectivity is only weakly dependent on the bulk phase composition, even at pore loadings close to the saturation loading. Similar results have been observed from experimental and simulation studies of CH₄/CF₄ adsorption in silicalite.¹²

In all three silica zeolites, the CO₂/N₂ selectivity increases as the bulk phase pressure is increased. This observation is most dramatic for ITQ-3 (see Figures 9 and 10), where the selectivity for $P > 10$ bar is more than double the (already large) selectivity in the limit of low pressure. IAST accurately predicts the initial rise in selectivity with pressure but does not correctly predict the plateau observed in the selectivity for $P > 10$ bar in Figure 9. The quantitative failure of IAST in this regime is not surprising, since when pore loadings become large, the ideality assumptions of IAST are likely to be poor. Systematic deviations of IAST from observed mixture data at high pressures have been observed elsewhere.^{8,12} The difficulty of applying IAST at high pressures is exacerbated by the fact that predicting mixture behavior in this regime requires information from the single-component isotherms at pressures much higher than the total pressure of the bulk mixture under consideration. That is, applying IAST at high pressures inevitably requires extrapolating fitted isotherms into regimes where no single-component data is available, especially for the less strongly adsorbed species in the adsorbed mixture.

As can be inferred from the single component adsorption isotherms, the CO₂/N₂ selectivity of these silica zeolites decreases dramatically as the temperature is increased. As shown in Figure 11, the selectivity of ITQ-3 is 10–20 times lower at 498 K than it is at room temperature. The decrease in selectivity is not as large in silicalite and ITQ-7, since these materials have smaller isosteric heats of adsorption than ITQ-3. Nonetheless, the ordering of the three materials in terms of their CO₂/N₂ selectivities (ITQ-3 > silicalite > ITQ-7) is the same at room temperature and 498 K.

4. Concluding Remarks

We have used atomistic simulations to examine the single-component and mixture adsorption of CO₂ and N₂ in three siliceous zeolites: silicalite, ITQ-3, and ITQ-7, at room temperature and at 498 K. The atomistic model we have used gives good agreement with room temperature single component isotherms, and the loading-dependent isosteric heat of adsorption in silicalite, the only material of the three we have studied for which experimental data is available. Our predictions for ITQ-3 and ITQ-7 are based on the reasonable, albeit untested, assumption that the intermolecular parameters determined for adsorption in silicalite are directly transferable to other siliceous zeolites.

All three of the zeolites we examined preferentially adsorb CO₂ over N₂ during both single-component and mixture adsorption. This phenomenon is due largely, although not exclusively, to the larger quadrupole moment of CO₂, which strengthens the Coulombic interactions between adsorbed molecules and the electric field of the zeolite. This observation suggests that the adsorption selectivity for CO₂ over N₂ might be enhanced in cationic aluminosilicalite zeolites, since these materials exhibit stronger local electric fields than the siliceous materials we have considered. The different electric fields present inside zeolites with different crystal structures play an important role in the observed adsorption capacities and selectivities. When only dispersion interactions are considered, the adsorption capacity and selectivity of the three materials we have considered are essentially equivalent in the limit of low pressures (see Figure 6a). At high pressures, silicalite shows a lower adsorption capacity for CO₂ than either ITQ-3 or ITQ-7, which exhibit approximately the same capacity when only dispersive interactions are considered. These observations correlate well with our estimations of the available void volume inside each material, which show that silicalite has the smallest void volume while ITQ-3 and ITQ-7 have similar void volumes. Once Coulombic interactions are included, the three zeolites show markedly different adsorption isotherms at both low and high pressures (see Figure 2). The very strong adsorption of CO₂ on ITQ-3 at low pressures and the very high CO₂/N₂ selectivities observed in this material are a result of the favorable electric field created by this crystal structure. Unfortunately, as we noted above, this explanation of the variation in adsorption selectivity between materials is difficult to use in a predictive sense since we know of no way to predict the net electric field of a zeolitic material without performing the detailed atomistic simulations described in this paper.

One important use for atomistic simulations of adsorption in microporous materials is to test the validity of models for multicomponent adsorption, such as the ideal adsorbed solution theory. We have examined the predictions of IAST for CO₂/N₂ mixtures in silicalite, ITQ-3, and ITQ-7 by comparing binary mixture GCMC results with IAST calculations based on isotherms fitted to our single-component GCMC simulations. We find that IAST performs quite accurately for these adsorbed mixtures. In particular, IAST correctly predicts the increase in CO₂/N₂ selectivity with increasing bulk pressure that is observed in each material, both at room temperature and at 498 K. The apparent validity of IAST can be understood by observing from the single-component heats of adsorption that the adsorption sites available for CO₂ and N₂ as a function of loading are relatively homogeneous. As a result, the main physical effect that occurs during mixture adsorption is that adsorbed CO₂ blocks sites in which N₂ would adsorb as a single component. This leads to mixture isotherms in which the amount of CO₂ adsorption is almost unchanged from the analogous single-component isotherm, while the amount of N₂ adsorbed is strongly suppressed relative to its single-component value (see Figure 8).

The CO₂/N₂ selectivities observed in the three siliceous zeolites we have modeled vary strongly as the crystal structure of the adsorbant changes. At room temperature, the observed selectivities in ITQ-7, silicalite, and ITQ-3 are approximately 10, 30, and 100, respectively. These results, combined with the high selectivities observed experimentally by Siriwardane et al.² in cationic aluminosilicalite zeolites, suggest that by appropriate choices of the pore structure and chemical composition it

should be possible to develop zeolites that have very favorable properties for CO₂-selective adsorption from mixed gas streams.

Acknowledgment. This work was funded in part by the U.S. DOE through the National Energy Technology Laboratory. D.S.S. is an Alfred P. Sloan fellow and also acknowledges the support of an NSF CAREER award (CTS-9983647). Computations were performed on a computer cluster supported by the NSF (CTS-0094407) and Intel. We thank Anastasios Skoulidas for many helpful discussions. D.K. and D.S.S. are delighted to acknowledge the influence that John Tully has had on their approaches to scientific and nonscientific issues. We dedicate this paper to John on the occasion of his 60th birthday.

References and Notes

- (1) Yang, R. T. *Gas separation by adsorption processes*; Imperial College Press: London, 1997.
- (2) Siriwardane, R. V.; Shen, M.-S.; Fisher, E. P.; Poston, J. A. *Energy Fuels* **2001**, *15*, 279.
- (3) Fuchs, A. H.; Cheetham, A. K. *J. Phys. Chem. B* **2001**, *105*, 7375.
- (4) Sircar, S. *Ind. Eng. Chem. Res.* **2002**, *41*, 1389.
- (5) Ko, D.; Moon, I.; Choi, D.-K. *Ind. Eng. Chem. Res.* **2002**, *41*, 1603.
- (6) Dunne, J. A.; Myers, A. L. *Chem. Eng. Sci.* **1994**, *49*, 2941.
- (7) Snurr, R. Q.; Bell, A. T.; Theodorou, D. N. *J. Phys. Chem.* **1993**, *97*, 13742.
- (8) Challa, S. R.; Sholl, D. S.; Johnson, J. K. *J. Chem. Phys.* **2002**, *116*, 814.
- (9) Clark, L. A.; Snurr, R. Q. *Chem. Phys. Lett.* **1999**, *308*, 155.
- (10) Golden, T. C.; Sircar, S. *J. Colloid Interface Sci.* **1994**, *162*, 182.
- (11) Sun, M. S.; Shah, D. B.; Xu, H.; Talu, O. *J. Phys. Chem. B* **1998**, *102*, 1466.
- (12) Heuchel, M.; Snurr, R. Q.; Buss, E. *Langmuir* **1997**, *13*, 6795.
- (13) Bowen, T. C.; Falconer, J. L.; Noble, R. D.; Skoulidas, A. I.; Sholl, D. S. *Ind. Eng. Chem. Res.* **2002**, in press.
- (14) Hirotsu, A.; Mizukami, K.; Miura, R.; Takaba, H.; Miya, T.; Fahmi, A.; Stirling, A.; Kubo, M.; Miyamoto, A. *Appl. Surf. Sci.* **1997**, *120*, 81.
- (15) June, R. L.; Bell, A. T.; Theodorou, D. N. *J. Phys. Chem.* **1990**, *94*, 8232.
- (16) June, R. L.; Bell, A. T.; Theodorou, D. N. *J. Phys. Chem.* **1990**, *94*, 1508.
- (17) Makrodimitris, K.; Papadopoulos, G. K.; Theodorou, D. N. *J. Phys. Chem. B* **2001**, *105*, 777.
- (18) Skoulidas, A. I.; Sholl, D. S. *J. Phys. Chem. B* **2001**, *105*, 3151.
- (19) Olson, D. H.; Kokotailo, G. T.; Lawton, S. L.; Meier, W. M. *J. Phys. Chem.* **1981**, *85*, 2238.
- (20) Cambor, M. A.; Corma, A.; Lightfoot, P.; Villaescusa, L. A.; Wright, P. A. *Angew. Chem., Int. Ed. Engl.* **1997**, *36*, 2959.
- (21) Villaescusa, L. A.; Barret, P. A.; Cambor, M. A. *Angew. Chem., Int. Ed. Engl.* **1999**, *38*, 1997.
- (22) Cook, S. J.; Chakraborty, A. K.; Bell, A. T.; Theodorou, D. N. *J. Phys. Chem.* **1993**, *97*, 6679.
- (23) Lonsinger, S. R.; Chakraborty, A. K.; Bell, A. T.; Theodorou, D. N. *Catal. Lett.* **1991**, *11*, 209.
- (24) Potoff, J. J.; Siepmann, J. I. *AIChE J.* **2001**, *47*, 1676.
- (25) Harris, J. G.; Yung, K. H. *J. Phys. Chem.* **1995**, *99*, 12021.
- (26) Allen, M. P.; Tildesley, D. J. *Computer Simulations of Liquids*; Oxford Science Publications: Oxford, 1994; p 133.
- (27) Frenkel, D.; Smit, B. *Understanding Molecular Simulation: From Algorithms to Applications*; Academic Press: London, 1996; p 381.
- (28) Allen, M. P.; Tildesley, D. J. *Computer Simulations of Liquids*; Oxford Science Publications: Oxford, 1994; p 349.
- (29) *Chemical Engineer's Handbook*, 5th ed.; Perry, R. H., Chilton, C. H., Eds.; McGraw-Hill: New York, 1973.
- (30) Karavaia, F.; Myers, A. L. *Langmuir* **1991**, *7*, 3118.
- (31) Vuong, T.; Monson, P. A. *Langmuir* **1996**, *12*, 5425.
- (32) Nicholson, D.; Parsonage, N. G. *Computer Simulations and the Statistical Mechanics of Adsorption*; Academic Press: New York, 1982.
- (33) Frenkel, D.; Smit, B. *Understanding Molecular Simulation: From Algorithms to Applications*; Academic Press: London, 1996; Appendix B.
- (34) Watanabe, K.; Austin, N.; Stapleton, M. R. *Mol. Sim.* **1995**, *15*, 197.
- (35) Talu, O.; Myers, A. M. *AIChE J.* **2001**, *47*, 1160.
- (36) Vitale, G.; Mellot, C. F.; Bull, L. M.; Cheetham, A. K. *J. Phys. Chem.* **1997**, *101*, 4559.
- (37) Macedonia, M. D.; Moore, D. D.; Maginn, E. J. *Langmuir* **2000**, *16*, 3823.
- (38) Jaramillo, E.; Auerbach, S. M. *J. Phys. Chem. B* **1999**, *103*, 9589.
- (39) Myers, A. L.; Prausnitz, J. M. *AIChE J.* **1965**, *11*, 121.
- (40) Jensen, C. R. C.; Seaton, N. A. *Langmuir* **1996**, *12*, 2866.